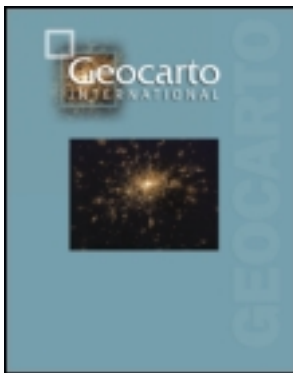


This article was downloaded by: [University of Ottawa]

On: 10 January 2012, At: 11:22

Publisher: Taylor & Francis

Informa Ltd Registered in England and Wales Registered Number: 1072954 Registered office: Mortimer House, 37-41 Mortimer Street, London W1T 3JH, UK



Geocarto International

Publication details, including instructions for authors and subscription information:
<http://www.tandfonline.com/loi/tgei20>

Remote sensing and GIS technology for studying lithospheric processes in a mountain environment

Michael P. Bishop ^a, John F. Shroder Jr. ^a, Valerie F. Sloan ^b, Luke Copland ^c & Jeffrey D. Colby ^d

^a Department of Geography and Geology, University of Nebraska at Omaha, Omaha, NE, 68182, U.S.A.

^b INSTAAR, University of Colorado, Boulder, CO, 80309, U.S.A.

^c Department of Earth and Atmospheric Sciences, University of Alberta, Edmonton, Alberta, T6G 2E3, Canada

^d Department of Geography, East Carolina University, Greenville, NC, 27858, U.S.A.

Available online: 17 Sep 2008

To cite this article: Michael P. Bishop, John F. Shroder Jr., Valerie F. Sloan, Luke Copland & Jeffrey D. Colby (1998): Remote sensing and GIS technology for studying lithospheric processes in a mountain environment, *Geocarto International*, 13:4, 75-87

To link to this article: <http://dx.doi.org/10.1080/10106049809354667>

PLEASE SCROLL DOWN FOR ARTICLE

Full terms and conditions of use: <http://www.tandfonline.com/page/terms-and-conditions>

This article may be used for research, teaching, and private study purposes. Any substantial or systematic reproduction, redistribution, reselling, loan, sub-licensing, systematic supply, or distribution in any form to anyone is expressly forbidden.

The publisher does not give any warranty express or implied or make any representation that the contents will be complete or accurate or up to date. The accuracy of any instructions, formulae, and drug doses should be independently verified with primary sources. The publisher shall not be liable for any loss, actions, claims, proceedings, demand, or costs or damages whatsoever or howsoever caused arising directly or indirectly in connection with or arising out of the use of this material.

Remote Sensing and GIS Technology for Studying Lithospheric Processes in a Mountain Environment

Michael P. Bishop and John F. Shroder Jr.

Department of Geography and Geology, University of Nebraska at Omaha
Omaha, NE 68182, U.S.A.

Valerie F. Sloan

INSTAAR, University of Colorado
Boulder, CO 80309, U.S.A.

Luke Copland

Department of Earth and Atmospheric Sciences, University of Alberta
Edmonton, Alberta T6G 2E3, Canada

Jeffrey D. Colby

Department of Geography, East Carolina University
Greenville, NC 27858, U.S.A.

Abstract

Analysis of relationships between uplift and denudation in complex mountain environments requires integrated approaches using remote sensing and geographic information systems (GIS) analyses in combination with field investigations. We present multidisciplinary research focusing on the Nanga Parbat Himalaya of northern Pakistan. Remote sensing of the subsurface includes radio-echo sounding to investigate glaciers, magnetotelluric sounding, and seismic tomography to investigate shallow to deep aspects of the lithosphere. Remote sensing of the landscape includes satellite image acquisition, multispectral analysis, geomorphometric analysis of a satellite-derived digital elevation model (DEM), and the application of GIS and pattern recognition procedures to analyze topographic complexity and the geomorphology of the mountain massif. Detailed mapping requires topographic normalization of satellite imagery using the non-Lambertian model. Radar measurement of thicknesses of glacier ice, coupled with assessment of satellite imagery and field data, have enabled calculation of ice and sediment discharge. Collectively, scientific observations reinforce prior understandings of rapid rates of uplift and high rates of surficial denudation. The integration of data has thus enabled a systematic approach to study localized coupling between tectonic and surface processes. In future studies of this kind, it will become ever more important for geoscientists to integrate quantitative remote sensing and GIS into a standard analytical framework in order to solve complex problems.

Introduction

The morphology and hypsometry of mountain environments is a result of the complex interaction of tectonics, climate, and erosional processes (Masek *et al.*, 1994; Avouac and Burov, 1996; Pinter and Brandon, 1997). Recent research indicates that surface erosion affects tectonic processes and may be a controlling force in mountain building (Pinter and Brandon, 1997). This is partly because intensive localized erosion causes rapid exhumation leading to thermal weakening of the crust and further concentration of strain (Zeitler, *et al.*, 1998), and partly because high rates of denudation result in a reduction of lithospheric mass which can cause isostatic uplift (Montgomery, 1994). As uplift increases elevation, climate change and glaciation can

significantly alter the topography and further reduce lithospheric mass, thereby increasing topographic relief even more (Molnar and England, 1990; Raymo and Ruddiman, 1992). The dynamic relationships between uplift and denudation are poorly understood, however, and there is a need to develop and evaluate models of landscape evolution that will explain scale-dependent topographic variation.

Landscape modeling requires a multidisciplinary approach, and is complicated by the fact that landform generating processes operate over a wide range of spatial and temporal scales (Molnar and England, 1990; Raymo and Ruddiman, 1992). Currently, we do not know the spatial or temporal scale-dependencies associated with many processes active in mountain environments (Shroder and Bishop, 1998a). Consequently, the issue of scale in spatial analysis

and integration of data into quantitative models are active research areas (e.g., Bian, 1997; DeFries *et al.*, 1997; Friedl, 1997), with developments in remote sensing and geographic information science providing new information and capabilities (e.g., Cao and Lam, 1997; Pecknold *et al.*, 1997; Quattrochi *et al.*, 1997).

Geoscience investigations of landscape evolution are best achieved with the use of remotely sensed data and GIS technology for data inventory and management, spatial analysis, and quantitative modeling. Digital elevation models (DEMs) and satellite multispectral data are necessary for studying the structural geology and surface geomorphology. Remote sensing of the subsurface is required to provide information regarding seismic activity and structures within the lithosphere. In addition, complex analysis and modeling are required for detailed mapping and the production of estimates of surface process rates. Numerous investigators have reported on the difficulties associated with data acquisition, numerical analysis, and information extraction from remotely sensed data in mountain environments (e.g., Franklin and Wilson, 1992; Gong, 1996). In the Himalaya, where rapid uplift and denudation produce extreme topographic relief, remote sensing and GIS technologies play a crucial role in assessing and understanding this complicated and dynamic system.

The purpose of this paper is to report current results and address the issues, approaches, and problems associated with studying lithospheric processes using remote sensing and GIS. We specifically report summaries and details of selected research projects at Nanga Parbat in Pakistan. Preliminary results include discussion of radio-echo sounding of glaciers, seismic tomography, magnetotelluric profiling, topographic normalization of satellite imagery, and geomorphometry.

The Nanga Parbat Project: An Overview

The Nanga Parbat massif, a knife-edged east-west trending ridge 8125 m high, stands out alone from the main Himalaya and Karakoram ranges in northern Pakistan (Figure 1). The mountain has been of great interest to western explorers since the nineteenth century. Many climbers have attempted the peak, but it was not until the 1930's that significant geological and geographical investigations, coupled with detailed (1 :50,000) cartographic mapping, were undertaken during German climbing expeditions. With the opening of the Karakoram Highway past the northern base of the mountain in the early 1980's, scientific research on the mountain began in earnest.

Research in the Hunza and Gilgit valleys to the north of Nanga Parbat enabled the extension of a Quaternary chronology to the mountain (Shroder *et al.*, 1989; Shroder *et al.*, 1993). Zeitler (1985) used fission-track dating of bedrock to determine exceptionally rapid rates of uplift and erosional unroofing of the massif of $\approx 10 \text{ mm yr}^{-1}$ over the past few million years. In addition, structural geologists discovered the major Raikot fault along the Indus River trench to the NE

of the mountain, along which uplift appears to be concentrated (Lawrence and Ghauri, 1983; Lawrence and Shroder, 1984; Madin, 1986). Since then, more extensive scientific exploration of the massif has confirmed that crustal and surface processes have been exceptionally active throughout the Quaternary Period (e.g., Butler and Prior, 1988; Coward *et al.*, 1986; Owen, 1988; Treloar *et al.*, 1989).

The Nanga Parbat Project is primarily supported by the Continental Dynamics Program of the U.S. National Science Foundation. The project was initiated by P.K. Zeitler to assess the recent and still active tectonic processes responsible for the extraordinary episode of very young, high-grade metamorphism, partial melting, high fold and fault strain, and rapid denudation focused around the center of the mountain. Fieldwork was initiated in 1995 to determine which crustal and surface processes were most instrumental in the development of Nanga Parbat during the collision of the Indian subcontinent with Asia. More than 20 investigators and students from a variety of disciplines and countries have collaborated to integrate into a geodynamic framework measurements made using petrology, geochronology, stable-isotope geochemistry, radiogenic tracer-isotope geochemistry, structural geology, radiocarbon, cosmogenic isotope and thermoluminescence dating, geomorphology and physical modeling. In addition, remote sensing of the surface and subsurface has included ice penetrating radio-echo sounding, magnetotelluric depth profiling, seismic tomography, satellite multispectral analysis, and satellite stereoscopy for production of a high resolution digital elevation model. With a diversity of data sets and significant data volume, a strong GIS approach to data collection, analysis, and portrayal has been required. Using this multidisciplinary approach, the group has begun to: (1) characterize the current state and evolution of the Indian crust making up the Nanga Parbat massif; (2) document the processes responsible for this evolution; and (3) combine this information into a coherent model applicable to other orogens. Our research activities focus on the remote sensing, GIS and geomorphology of the upper portion of the lithosphere.

Remote Sensing of the Subsurface

A variety of structures and rock types occur beneath Nanga Parbat. The generation of granite in the Himalaya range has been typically viewed as a relatively deep-seated phenomenon, largely divorced in time and process from the relief-cutting phase in which the high peaks grew. Nanga Parbat, however, may be sitting astride or near melt zones as the strong denudation observed on the mountain may have caused decompression melting at depth and injection of young leucogranites now exposed by erosion at the surface (Zeitler and Chamberlain, 1991; Zeitler, *et al.*, 1993). The present-day temperature and rheologic condition of the crust beneath the mountain are thus of great interest. Seismic tomography and magnetotelluric depth sounding have enabled an examination of the lithosphere at depth.



Figure 1 LANDSAT MSS false color composite of Nanga Parbat. False color composite was generated using MSS band 6 (red), MSS band 5 (green), and MSS band 4 (blue). Image width represents ~ 60 km. In general, snow appears white, bare glacial ice appears light blue, bare bed rock and rock detritus appear brown and dark blue, and vegetated surfaces appear in shades of red. The Indus River and valley are located in the upper left portion of the image. The Astor River and valley are located on the east side of Nanga Parbat. Alpine glaciers are found in most basins surrounding the mountain.

Seismic Tomography

Seismic waves, the transmission of energy from the focus of an earthquake shock, occur as a number of different wave forms that travel through the Earth at different speeds. The fastest are the primary waves (P) that are identical in character to sound waves passing through a liquid or a gas. A slower form are secondary waves (S) that oscillate back and forth at right angles to the direction of propagation. Both produce seismic vibrations which are expanding spheres of wave-front energy in which seismic rays, or lines perpendicular to the wave front, would be straight lines in a homogeneous body. The Earth is not homogeneous, however, which causes the rays to be reflected and refracted. Furthermore, P waves travel through both solids and liquids, whereas S waves are damped out in liquids. Additionally, cold rock tends to be more rigid and incompressible than hot material, which means that seismic waves traverse cold regions of the crust more rapidly. Conversely, hot material decreases seismic velocities, with molten fluid possibly attenuating part of the signal altogether.

Seismic tomography (Anderson and Dziewonski, 1984), as with its medical analog, the computer-aided tomography or CAT scan, combines information from a large number of directional energy sources to construct three-dimensional views of the medium the rays have traversed. With the aid of a computer, large numbers of cross-sectional views are integrated to produce a three-dimensional view. In seismic tomography, the velocities of hundreds of thousands of seismic waves are used to analyze the character of the rock through which they are passing, and to thereby construct temperature profiles at depth.

In the case of Nanga Parbat, the best available source of seismic energy comes from the wide variety of earthquake-generating features in the crust at distances of up to several hundred kilometers from the massif. Records from seismographs installed during this project throughout the massif and its periphery are now being analyzed by the seismology group (directed by A. Meltzer) to determine the condition of the Earth's crust beneath the mountain. Preliminary analyses of the seismic data gathered to date show locations, focal mechanisms, and many waveforms indicative of an area of anomalous velocity structure beneath the massif (A. Meltzer, personal communication, 1997). This area is small in size, however, with apparently no large magma bodies present, although there may be smaller zones of partial melt, or at least very hot rock. Various models with shallow and deep melt zones and various fault characteristics are now being tested to further reconcile observational data with possible rock and melt configuration at depth.

Magnetotelluric Profiling

According to the principle of electromagnetic induction, alternating electric currents have an associated alternating magnetic field. In this case, fluctuating ionospheric currents, fixed with respect to the sun, and correlative with diurnal changes in the Earth's magnetic field, induce natural or telluric currents that flow in large sheets everywhere on and within the surface of the Earth (Dobrin, 1976; Sharma, 1986). The current distribution at any one place depends upon the resistivity of the rocks encountered. Conductivity is highly sensitive to the presence of free water in the crust, whether in crustal melts or not. Dry melting results in a resistive magma that cannot be detected by magnetotellurics. Magnetotelluric surveying, however, is generally capable of detecting shallow, wet magma bodies, fluid-saturated zones, and fluids derived from deep-seated sources. In addition, the internal characteristics of great thicknesses of alluvial sediments in basins and troughs are also detectable.

Results of the magnetotelluric analysis at Nanga Parbat (Park and Mackie, 1998a) show that shallow crustal (< 10 km) conductors correlate with a hydrothermally altered Raikot fault zone and/or carbonaceous metamorphic rocks near the Raikot fault on the northwest side of the range. Chamberlain *et al.* (1995) showed that the hydrothermal system at Nanga Parbat consists of a shallow system dominated by meteoric water and a deeper system with metamorphic and/or magmatic waters. Hydrogen and oxygen isotope values in hot springs

along the Raikot Fault suggest that the hot fluids result from deep circulation of glacial meltwaters driven by the steep topographic gradient on the north face of the massif. The magnetotelluric data are consistent with this interpretation and suggest that fluids do not circulate too deeply along the Raikot Fault. In an initial analysis, a prominent mid-crustal conductor appeared to be located directly beneath Nanga Parbat, but its exact depth, dimensions, and conductivity were poorly constrained by the existing data. The magnetotelluric data seemed consistent with a wet and conductive magma at the depth of the mid-crustal conductor, although further work by the magnetotelluric group (directed by S. Park) was required to identify it with certainty.

When used together, magnetotellurics and seismic tomography can identify zones of melt beneath the Nanga Parbat massif, whether dry or wet, because they will be seismically slow and resistive when dry, as opposed to slow and conductive when wet. Consequently, identification and mapping of decompression melting and metamorphism at Nanga Parbat is possible. When combined with data from satellite and terrain analysis, GIS overlay analysis improves our understanding of denudation-induced decompression melting.

Radio -Echo Sounding and Ice Motion Determination

Information regarding surface denudation rates involves evaluating the contributions of the fluvial, mass movement and glacial erosion components of the geomorphic system. It has been argued that glaciation is one of the most powerful erosional agents on the landscape (Molnar and England, 1990; Harbor and Warburton, 1993; Hallet *et al.*, 1996). Consequently, information regarding glacier distribution, ice depths, ice velocities and debris content is required to determine ice discharge and glacial denudation rates from sediment fluxes.

At Nanga Parbat a variety of techniques have been integrated to produce estimates of contemporary rates of glacial denudation on the massif. In the summers of 1996 and 1997, surface ice velocities were measured at a series of cross-glacier transects in the ablation area of seven of the main glaciers flowing from the mountain (Raikot, Buldar, Chongra, Bazhin, Tap, Shaigiri and Rupal glaciers). These velocities were determined by surveying the location of markers painted on boulders at the start and end of periods ranging from three to six days with a Geodimeter electronic theodolite. These measurements have an accuracy of ± 7 - 24 mm over the distances surveyed, and provide detailed information regarding the spatial velocity distribution at a variety of locations. In addition, surface velocity measurements made by several previous researchers (e.g., Finterswalder, 1937; Pillewizer, 1956; Gardner and Jones, 1993) were used to supplement and extend the coverage of these measurements.

To enable accurate calculations of the volume of debris being transported by a glacier, it is also necessary to know the supraglacial debris depth, englacial debris volume, and ice thickness. As is typical of most Himalaya glaciers, the

ablation areas of the glaciers around Nanga Parbat are generally covered by unconsolidated material to a thickness of several meters or more. This debris thickness is measured by digging through the debris layer until solid ice is reached, and then measuring the depth to the ice from the debris surface. Based on observations of supraglacial debris exposed in ice cliffs at the margins and over the surface of the glacier, a debris depth of 1.5 m was recorded when the debris was too thick to enable the underlying ice to be reached. Englacial debris volumes were determined by taking ice samples from exposed surface ice cliffs in the ablation area, melting the ice, filtering the resulting water, and then finding the dry weight of the sediment on the filter paper. It was assumed that locations closer to the glacier terminus represent ice that was originally at a greater depth within the glacier.

Point measurements of ice thickness were made with the use of a portable radio-echo sounding (RES) system at a center frequency of 5 MHz. Also called ground-penetrating radar, RES is an active geophysical technique that is being increasingly used to investigate the internal and basal structure of glaciers and ice sheets. The physical basis of RES relies on the fact that the propagation of electromagnetic waves varies according to the electrical properties of the medium. The dielectric constant of a medium defines the speed of propagation, and consequently changes in the dielectric constant at the interface between materials (e.g., at the interface between glacier ice and bedrock/sediment) produce reflections of the transmitted signal that can be detected at the glacier surface.

There has been only limited previous use of RES in the Himalaya (e.g., Oswald, 1984) due to the inaccessibility of the area, the bulkiness of previous systems, and poor bed reflections caused by the radar waves being dissipated by the thick supraglacial debris cover. Many of these problems were overcome at Nanga Parbat by using a lightweight portable RES system. This consisted of a high-powered pulse transmitter (Narod and Clarke, 1994), hand-held Tektronix THS oscilloscope receiver, HP 200 palmtop computer for data recording, portable solar panel and rechargeable batteries as a power source, and an altimeter and hand-held Garmin GPS to determine the location of the measurement points. After testing to determine the optimum system configuration, the transmitter and receiver arms were oriented in an up/down glacier direction, and separated by a cross-glacier distance of 20 m. Measurements of ice thickness were then made at approximately 60 locations over the ablation area of Raikot glacier, and at approximately 10 locations across each of two transects on Bazhin and Chongra glaciers.

The oscilloscope displayed the received energy at each location (a *trace*), with the final recorded trace representing the average of 15 seconds worth of readings to reduce noise. The bed reflection generally occurred as a distinct peak at a time of ≈ 1000 nanoseconds (ns) to 3500 ns from the surface air wave (Figure 2). If it is assumed that radar waves travel through ice at a velocity of 0.168 m ns^{-1} (Evans, 1965), then these times equate to a two-way travel distance of 168 m to

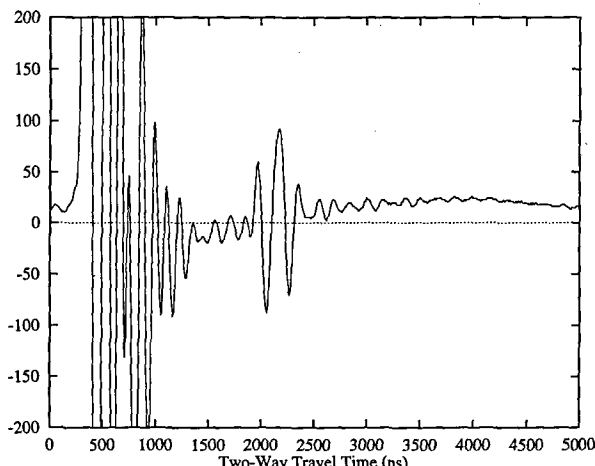


Figure 2 An example of a radio-echo sounding trace recorded at the 200 m location shown in Figure 3. Two-way travel time between the peak of the surface wave and the peak of the bed wave is 1840 ns, which equates to an ice thickness of 155 m.

588 m, or an ice depth of 84 m to 294 m. The resolution of the ice depth records is generally taken to be one third of the wavelength (Bogorodsky *et al.*, 1985), which equates to a resolution of approximately 11 m with a transmitter frequency of 5 MHz. It was usually easy to identify the bed location in the RES traces, and therefore enable reconstruction of the glacier bed topography (Figure 3).

When surface velocity, debris measurements, and glacier thicknesses are combined, an estimation of ice discharge and sediment transport rates is possible. For example, ice flux through the cross-section on Raikot glacier, illustrated in Figure 3, is calculated at $3.3 \times 10^6 \text{ m}^3 \text{ yr}^{-1}$ based on the surface velocity measurements made in 1996 (see Table 2, Shroder *et al.*, 1998b, for details). This flux was obtained by multiplying the mean surface velocity by the cross-sectional area of the transect, following the methodology outlined by Paterson (1994). Assuming that this part of Raikot glacier carries a mean internal sediment load of $2,125 \text{ mg l}^{-1}$ based on the analysis of 13 ice samples (Gardner and Jones, 1993), this equates to an englacial transport rate of 6,400 metric tons yr^{-1} . Measurements of supraglacial debris depth were also made at each surface velocity marker across the cross-section, which enables an estimation of the supraglacial debris transport rate. Assuming that the debris has a porosity of 0.30 and density of 2.5 (Gardner and Jones, 1993), then the supraglacial transport rate through this cross-section is 5,600 tons yr^{-1} , giving a total estimated debris transport rate through this cross-section of 12,000 tons yr^{-1} .

These calculations demonstrate that a variety of techniques provide effective estimates of glacial discharge and sediment transport rates at Nanga Parbat. Most previous studies in the Himalaya have been unable to provide accurate estimates of ice discharge due to the lack of information on ice depth (e.g., Gardner and Jones, 1993), but here it has been demonstrated that a lightweight RES system can provide detailed depth records even when the glacier surface is covered by up to a meter or more of unconsolidated debris.

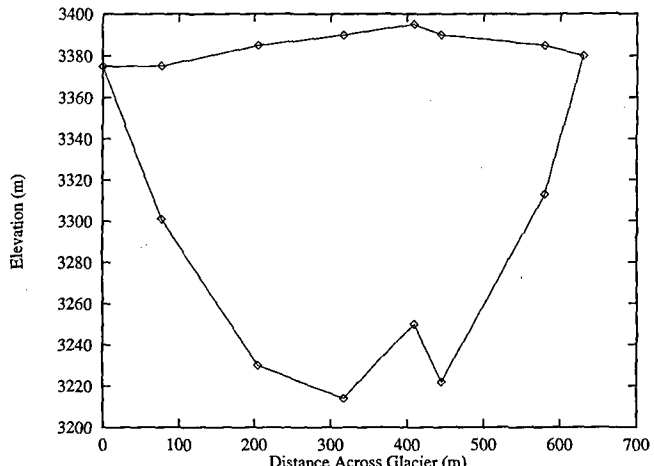


Figure 3 Ice thickness as determined by radio-echo sounding at the location of the main surface velocity transect on Raikot Glacier, approximately 2.5 km from the glacier terminus. View is in a downglacier direction.

These data, coupled with satellite image analysis, enable estimations of sediment transport rates, and consequently production of quantitative estimates of denudation.

Remote Sensing of the Landscape

Denudation modeling requires detailed information about topographic complexity and the geomorphology around Nanga Parbat. Satellite remote sensing is the only practical way to obtain detailed spatial information about the landscape, as logistical and physical limitations restrict access and field work, and aerial photography is effectively prohibited in Pakistan (Bishop *et al.*, 1995). Satellite multispectral imagery and DEM data must be integrated to assess topographic complexity and map landforms.

The detailed mapping of Nanga Parbat requires radiometric calibration of satellite imagery in order to correct for differential illumination. All multispectral data sets (i.e., LANDSAT MSS, LANDSAT TM, SPOT panchromatic and multispectral) exhibit a strong modulation of brightness due to topography. Consequently, it is imperative that we assess various reflectance models for topographic normalization as they have not been thoroughly evaluated in such extreme relief before.

Topographic Normalization

The natural surface variable, which exerts perhaps the strongest influence on remotely sensed data, is topography (Estes, 1983). Slope and aspect vary significantly over short distances in mountainous terrain. A wide range of effective illumination and view angles are, therefore, obtained for multispectral imagery (Smith *et al.*, 1980). This differential illumination of the surface is manifested visually as the impression of topographic relief and is frequently referred to as the topographic effect (Justice and Holben, 1979). Digital analysis of satellite imagery for extraction of thematic information in rugged terrain is impaired because spectral

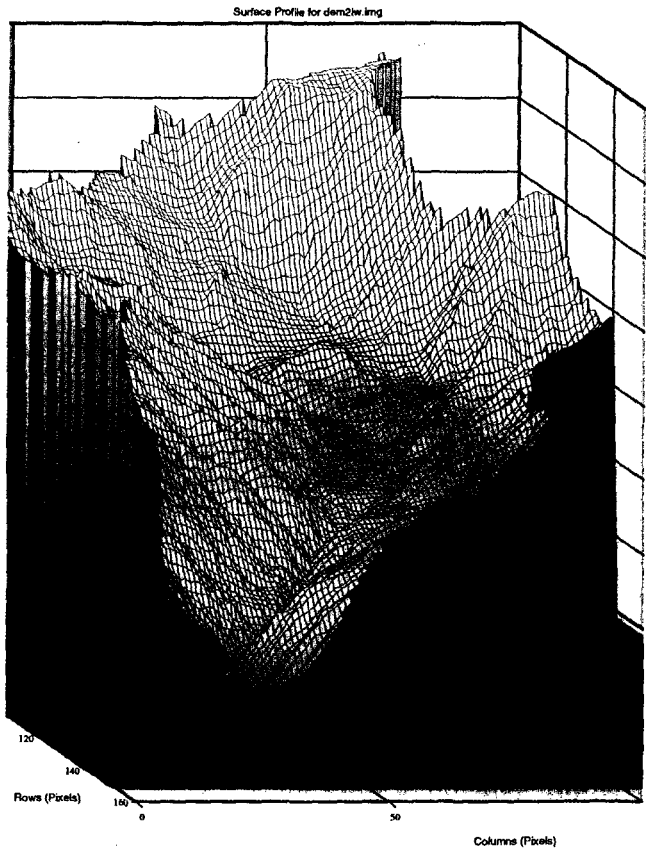


Figure 4 Surface of the Raikot Basin on the north side of Nanga Parbat. Surface profile was generated using a satellite derived digital elevation model. View is towards the south looking at the Nanga Parbat summit.

reflectance from a single cover type can vary with topography. Anisotropic reflectance, which is partly a function of surface cover, further confound the interpretation of multispectral imagery in mountainous terrain (Hugli and Frei, 1983).

Efforts have been made to minimize topographic effects on multispectral imagery (e.g., Smith *et al.*, 1980; Justice *et al.*, 1980; Teillet *et al.*, 1982; Hugli and Frei, 1983; Civco, 1989; Colby, 1991; Meyer *et al.*, 1993; Ekstrand, 1996; Colby and Keating, 1998). The Lambertian and non-Lambertian models have received significant attention in attempting to improve radiometric correction. In previous applications the non-Lambertian model has proven effective in reducing the influence of topographic effects in temperate (e.g., Colby, Meyer *et al.*, 1993), as well as tropical montane areas (Colby and Keating, 1998). Conversely, application of the Lambertian model has not been shown to be effective in reducing topographic effects in these locations.

Himalaya Example: Raikot Basin

The Lambertian and non-Lambertian models were evaluated to reduce topographic effects in SPOT multispectral imagery of Nanga Parbat. The topographic relief found in this area is extreme. For example, the relief in Raikot Basin ranges from 1100 - 8125 m over a horizontal distance of 21 km (Figure 4). Slope steepness and variability are extreme,

with an average slope angle of $\approx 32^\circ$ for most basins. Consequently, a strong modulation of brightness due to topography exists, and interpretation of satellite imagery is difficult. We wanted to determine the feasibility of using these models in extreme relief because this may be the first application of the non-Lambertian model to correct for topographic effects using SPOT multispectral imagery in the Himalaya.

Operation of the correction model required the integration of the multispectral imagery and digital elevation model (DEM) data. It is difficult to rectify images in mountainous environments. Typical problems include lack of large-scale maps and DEMs. Similarly, identifying quality control points is problematic due to the dynamic nature of the environment. At Nanga Parbat, monsoon precipitation, glaciation, and frequent mass movement, including rock falls, landslides, and debris flows, alter the land cover and topographic characteristics, making it difficult to identify static features. As a result, obtaining a reliable, large sample size is difficult. Ortho-rectification represents the best possible solution as relief displacement should be taken into consideration. SPOT Data Corporation produced a DEM and an ortho-rectified panchromatic image for the Nanga Parbat area using map control (1:50,000 German topographic map). The multispectral imagery was rectified using control points that could easily be identified in the multispectral imagery and ortho-rectified panchromatic imagery. The total root mean squared error was 4.28 m based on 25 control points. Ortho-rectification was not utilized as we received reasonable results for our preliminary assessment. We plan to ortho-rectify all imagery for detailed mapping and quantitative analysis in future studies.

The normalization process based on the non-Lambertian model includes application of a backwards radiance correction transformation (BRCT) (Smith *et al.*, 1980):

$$Ln = L(\cos e)/(\cos^k i \cos^k e) \quad (1)$$

where: L is radiance, e is the exitance angle (slope), i is the incidence angle, Ln represents the radiance when $i = e = 0$, and k is the Minnaert constant.

A modified version of the ERDAS Imagine algorithm developed by Hodgson and Shelley (1994) was utilized to normalize the SPOT multispectral band images based on the BRCT. Minnaert constants (Minnaert, 1941) were calculated separately using the $\cos i$, $\cos e$, and the three spectral band images (Colby and Keating, 1998). Investigating methods for the optimum derivation of Minnaert constants is an important facet of our work in order to improve our understanding of how to reduce the effects of topography and anisotropic reflectance.

Most previous applications of non-Lambertian models have focused on calculating Minnaert constants for separate cover types. Recent articles have shown the utility of calculating Minnaert constants for entire study areas in order to improve classification accuracy (Meyer, 1993; Colby and Keating, 1998).

Minnaert constants were calculated for the entire Raikot

Basin (Table 1), and then for both upper and lower portions of the basin. Inspection of the lower portion of the basin after normalization using Minnaert constants derived from the entire basin revealed a visible reduction of the topographic effect (Figures 5 and 6).

Table 1 Minnaert Constants calculated for the Raikot Basin.

SPOT Spectral Band	Minnaert Constant (k)
Band 1	0.4762
Band 2	0.3897
Band 3	0.4272

Initial quantitative assessments were undertaken based on a linear regression of the $\cos i$ values and corresponding spectral values after normalization. The results revealed a reduced relationship between $\cos i$ values and the spectral values which had been normalized, indicating a decrease in the topographic effect. The reduction in the relationship between $\cos i$ and normalized spectral values was more

prominent between values normalized using Minnaert constants derived separately for the upper and lower portions of the basin. This result is not surprising given the extreme complexity of the topography and cover types in the basin. Assessment of the Lambertian-corrected image of the lower basin indicated an increased relationship between illumination and spectral values as compared to the raw image. The results from application of the Lambertian model are consistent with previous research, suggesting it is not a useful correction method in areas of such rugged terrain. Ongoing efforts investigating the reduction of the effects of topography and anisotropic reflectance in our work include the development of alternative methods for calculating Minnaert constants and diagnostic methods for evaluating the effectiveness of their application.

Landscape Geomorphometry

Landscape geomorphometry, the quantitative characterization of terrain and landforms, is integral in the assessment of rates of denudation on Nanga Parbat massif. We are using geomorphometric analyses for quantitative modeling of rates of denudation, geomorphological mapping, assessing the volume of sediment stored on the massif, and in the reconstruction of the glacial, fluvial, and mass

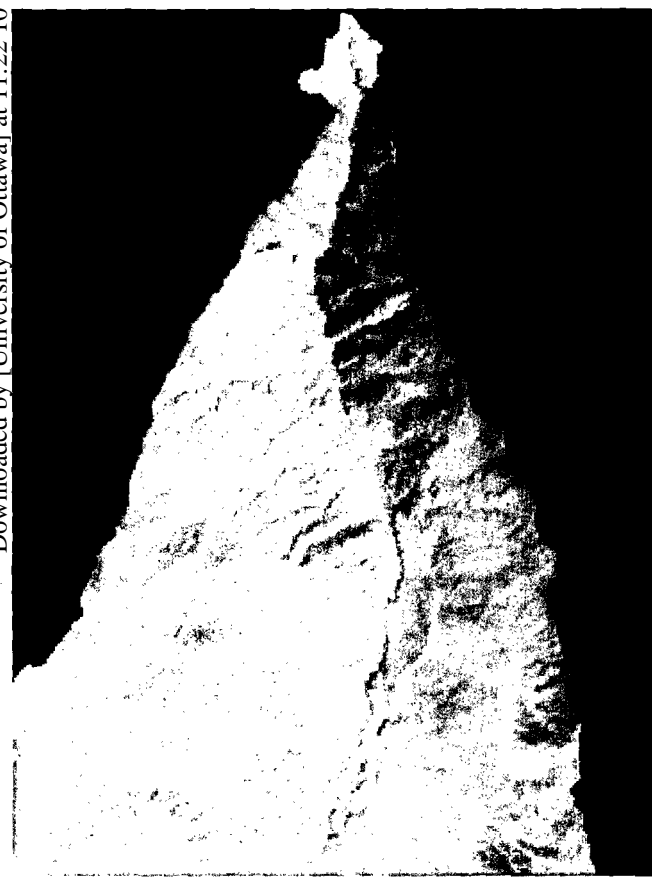


Figure 5 SPOT 3 spectral band 1 (0.50 - 0.59 μm) image of the lower portion of Raikot Basin. Image acquisition date is 6-9-1996 with a sun azimuth and elevation at 1 27.0 and 71.2 degrees respectively. Differential illumination is present at a variety of scales, however, the lowest frequency variation is not visible due to the applied contrast enhancement. Higher frequency reflectance variation is clearly visible and highlights the terrain. The terminus of the Raikot glacier can be seen in the lower central portion of the image.

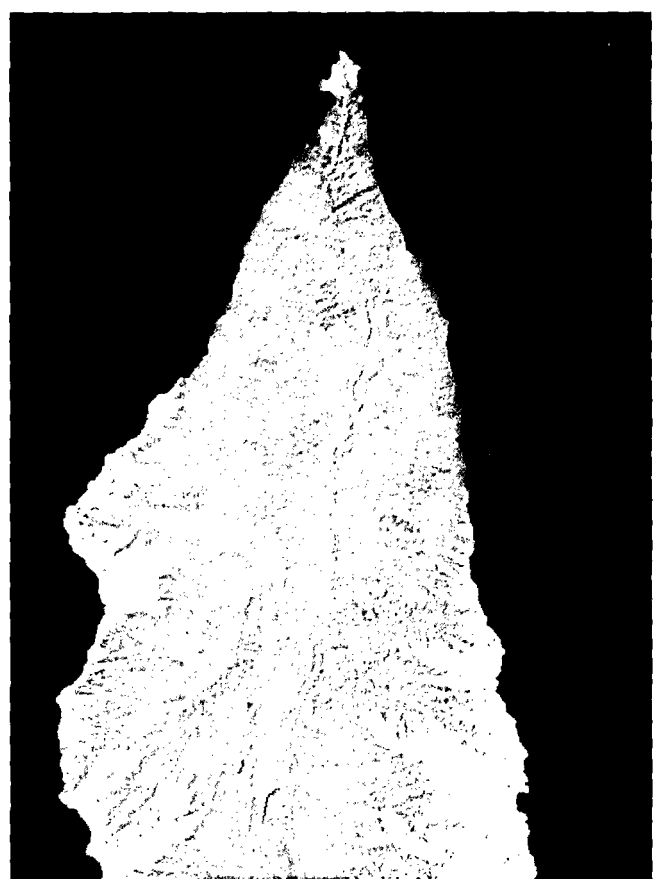


Figure 6 SPOT 3 spectral band 1 (0.50 - 0.59 μm) image of the lower portion of Raikot Basin after topographic normalization. Much of the higher frequency reflectance variability found in the original image (Figure 5) has been significantly reduced.

movement history. Additional analysis will focus on characterizing the scale-dependent nature of topographic variation in order to examine the relationships between tectonics and surface processes.

Digital Elevation Model

A SPOT panchromatic stereo-pair was acquired on 10-27-1996 and 10-28-1996. A digital elevation model (DEM) was generated by SPOT Data Corporation using the imagery and the stereoautocorrelation method (Figure 7). Spectral saturation was not a problem and good correlations were obtained at high altitudes. Topographic map coverage was used to construct the topography at the summit where spectral saturation did occur. This area was extremely small and represents an insignificant area with respect to mapping and analysis. A large sample of global and local control points from topographic maps of the region were used to ensure quality control. Separate control points were used to determine accuracy. The resolution is 20 m with a vertical accuracy of 8—12 m. The DEM covers a radius of ~ 30 km centered over Chongra Peak on the Nanga Parbat massif. Initial analyses of the DEM included hypsometric analysis, swath profile analysis, and slope analysis.

Swath Profiles Across Nanga Parbat Massif

Relief statistics were calculated for swaths across the DEM representing an area of 40000 x 20 m. This equates to calculating relief statistics using every pixel in a given row or column depending upon the profile direction. For example, statistics for a north-south profile were calculated from each row (40 km swath width). Statistics for a west-east profile

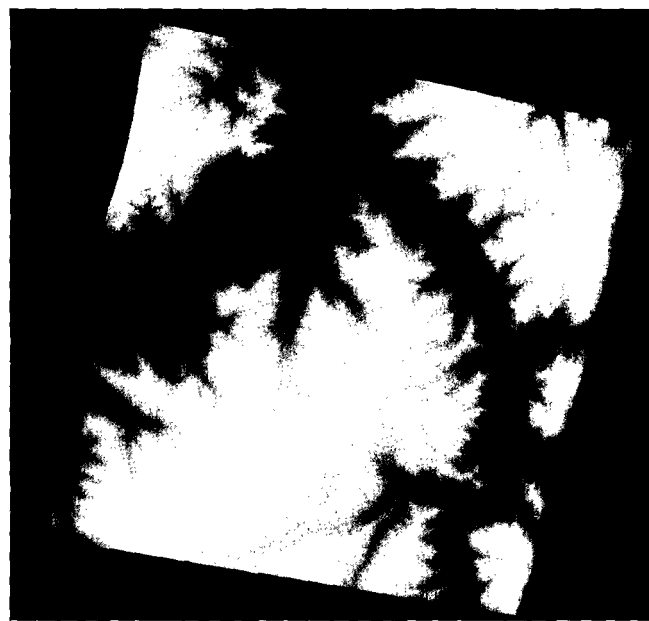


Figure 7 Digital elevation model (DEM) of the Nanga Parbat massif. The DEM was generated from SPOT panchromatic stereo pairs acquired on 10-27-1996 and 10-28-1996 using stereo-correlation procedures.

were calculated from each column (40 km swath width). The impressive topography across the Nanga Parbat massif is illustrated in Figure 8. The rate of change of maximum elevation and relief is roughly symmetrical about both sides of the summit. The mean elevation calculated for the profile ranges from 2500 - 4000 m.

A west-east topographic profile indicates that maximum elevation and relief changes rapidly across the massif, with a 3000 m increase across a 15 km distance (Figure 9). The maximum elevation change observed along this profile shows a more gradual gradient on the west side and an extremely steep slope on the east.

The minimum elevations across the massif reflect the depth of river incision, and illustrate local base level at the foot of the massif. The lower portion of the minimum elevation curves on both Figures 8 and 9 represent the Indus River, while higher elevations of the minimum curves represent the Astor River. The Astor River circumnavigates the Nanga Parbat to the east and flows into the Indus River. The gradient of the minimum elevation curve in Figure 8 shows a steep portion with a drop in altitude of greater than 1000 m over a horizontal distance of about 5 - 6 km. This steep segment may reflect the low elevations across a region of rapid uplift associated with the Raikot fault zone. Burbank *et al.* (1996) used dated strath terraces to measure differential river incision across the massif along the Indus River in the valley immediately to the north of the Astor valley. It is possible that this steep minimum elevation gradient shows that the river is seeking equilibrium and cutting back into the massif as the massif uplifts.

Slope Analysis

Slope angles were calculated from the digital elevation model using a least squared regression approach to produce mean slope angles over a 40 x 40 m area (Figure 10). Low slope angles generally occur in broad, flat valley floors in

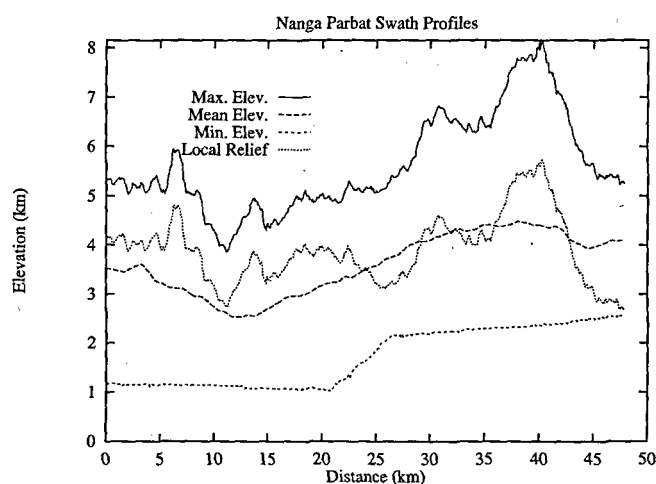


Figure 8 North-South topographic profile across the Nanga Parbat massif. Relief statistics were calculated from the DEM using a swath width of ≈ 40 km.

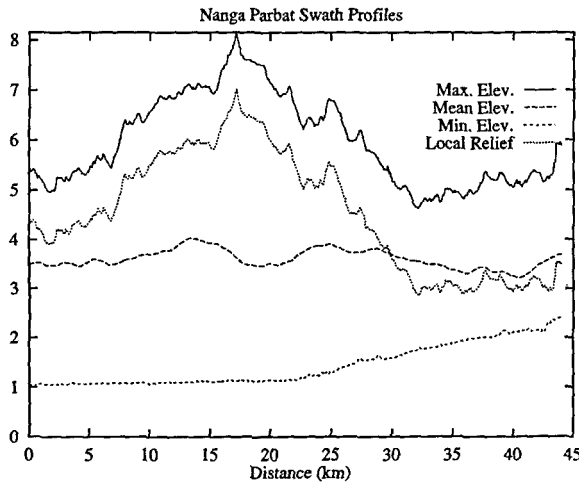


Figure 9 West-East topographic profile across the Nanga Parbat massif. Relief statistics were calculated from the DEM using a swath width of ≈ 40 km.

the glacially eroded valleys, whereas greater slope angles reflect steep and high faces, such as the Rupal face on the south side of the massif.

Slope distributions for Nanga Parbat and numerous basins were calculated (Figure 11) and show that the mean slope angle over the massif is $\approx 32^\circ$. A similar mean slope angle estimate was calculated by Burbank *et al.* (1996) for the same area using a DEM with a resolution of 90 m. Burbank *et al.* (1996) concluded from their observations of slope angles that slope failure triggered by river incision was the dominant geomorphic control on the topography of the landscape. Subsequently, however, their hypsometric analyses in the same regions were interpreted as demonstrating that glacial processes control the topography, regardless of the rate of uplift (Brozovic *et al.*, 1997). The relatively steep slopes on Nanga Parbat are likely due to a combination of these processes, with landsliding triggered by river incision causing slope steepening at lower elevations, and glacial headward erosion and freeze-thaw action creating steep slopes at higher elevations. Hypsometric analysis shows that significant mass has been removed, whereas field work provides evidence of polygenetic slope formation (Shroder *et al.*, 1998c).

Slope versus Altitude in the Raikot Basin

A plot of slope versus elevation calculated for Raikot basin shows dramatic slope variations with altitude (Figure 12). The maximum slope angles are consistently high. Maximum slopes taper off at the highest altitudes near the summit, at a small plateau called the Silver Saddle, and at the lowest altitudes where the basin reaches the broad and gently sloping Indus Valley. At lower elevations, above the Indus Valley, the mean slope angles rise dramatically to 45° at an elevation of 1700 m. This part of the Raikot basin is located along the southeastern side of the Indus valley, where the hanging valley of the Raikot opens out into the main trunk valley, and where the Raikot fault is located. The Nanga Parbat massif on the southeast side of this fault zone is

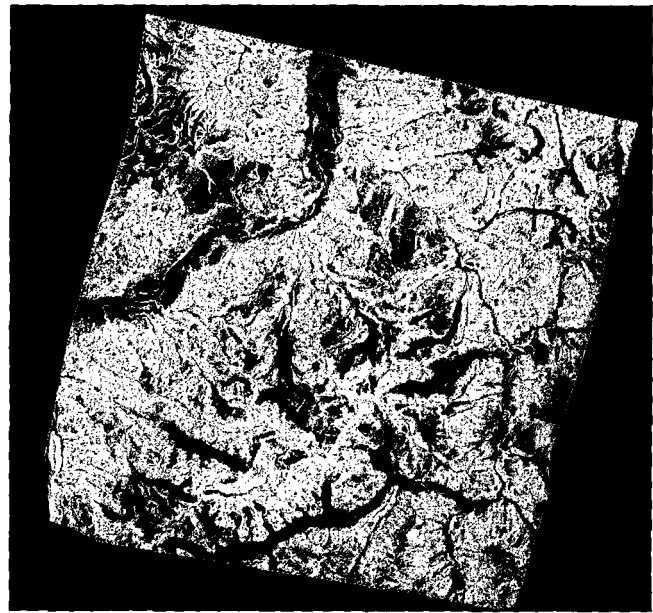


Figure 10 Slope angle map of the Nanga Parbat massif. Average slope angles were derived from the DEM over a 40×40 m area using a least squares regression analysis. Lower slopes are associated with valley bottoms and at higher elevations where glaciation has decreased topographic complexity.

uplifting rapidly in comparison to the terrain on the Indus side. Consequently, this zone of steep slopes may be a result of both glacial processes and the rapid thrust faulting along the Raikot fault. With increasing elevation up the basin, the mean slope angles decrease and then gradually increase. This middle zone of lower slope angles represents the creation of U-shaped valleys by glaciation. In higher reaches of the Raikot basin, mean slope angles increase to $\approx 50^\circ$.

Discussion

Remote sensing of the subsurface and surface of Nanga Parbat has produced a tremendous volume of new spatial data which should provide insights into the workings of this complex dynamic system. The working model suggested by a variety of investigators is that climate, and therefore surface processes, can play an important role in influencing tectonic processes and mountain building (Molnar and England, 1990; Hoffman and Grotzinger, 1993; Harrison, 1994). Rapid denudation would reduce lithospheric mass and induce isostatic uplift. Active tectonism is also thought to play a role, although, differentiating isostatic versus tectonic uplift is an extremely difficult task (England and Molnar, 1990; Montgomery, 1994). Key objectives of this research are to document uplift rates and the magnitude of modern-day and Quaternary denudation. Furthermore, it is important to document the nature of tectonism and erosion and identify complex feedback mechanisms.

To date, new understandings of rapid uplift and ferocious denudation at Nanga Parbat have been produced from remote sensing analyses. Remote sensing of the subsurface indicates that active seismicity is associated with the highest

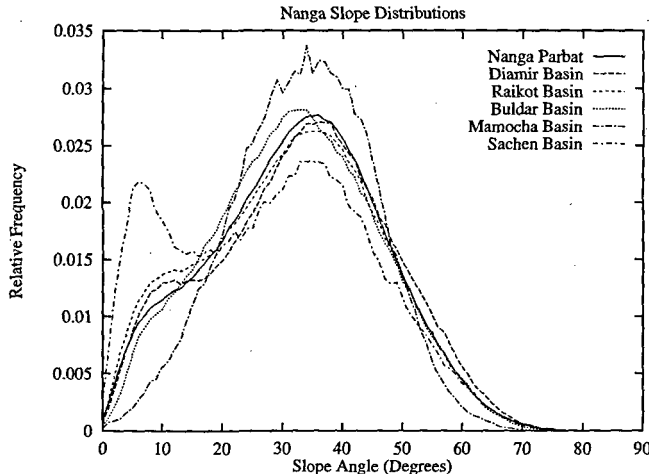


Figure 11 Slope distributions for Nanga Parbat and various basins around the mountain. The modal slope angles are $\approx 37^\circ$. The secondary peak of frequencies at $\approx 8^\circ$ represents the influence of glaciation on the landscape.

topography, youngest metamorphic and igneous ages, and active fluid flow, which suggests that fundamental processes link these factors. Furthermore, much of the observed seismicity is from a set of shallow normal faults on the northeast that strike roughly parallel to the main massif and dip south to southeast, back toward the summit. These normal faults may be the result of either small scale gravitational collapse or hydrofracturing associated with fluid injection at depth (Meltzer *et al.*, 1998). At ≈ 7 km depth beneath the mountain a cut-off in seismicity suggests a shallow transition from the characteristic deeper ductility of rock masses to a shallower brittle nature. Finally, the spatial distribution of the microseismicity also indicates rapid upward advection of rock material within the core of the massif (Zeitler *et al.*, 1998).

Additional analysis using a wider spread of magnetotelluric sensors (Park and Mackie, 1998b) showed no evidence of conductors directly beneath the highest topography, which ruled out watersaturated melts, or other circulation of fluids beneath the mountain, but not a dry zone of partial melts. Nevertheless, such a magma would have low velocities of compressional seismic waves, which were not observed, with the result that the proposed zones of partial melt beneath the mountain were also ruled out. Further work now in progress was then realized as necessary to reconcile the seismic and magnetotelluric data, and to explain the observed unusual heat flow and the petrologic and fluid-flow anomalies associated with the mountain. Various alternate hypotheses are now being considered, including lateral importation of rock along an upward ramp thrust of a partial melt zone from deeper to the southeast of the massif. These results, involving the combination of seismic analysis and magnetotellurics, together with conventional field mapping, visual interpretation of satellite imagery, and dating of bedrock on the surface, give us the best possible view of subsurface processes that have led to the enormous massif of today.

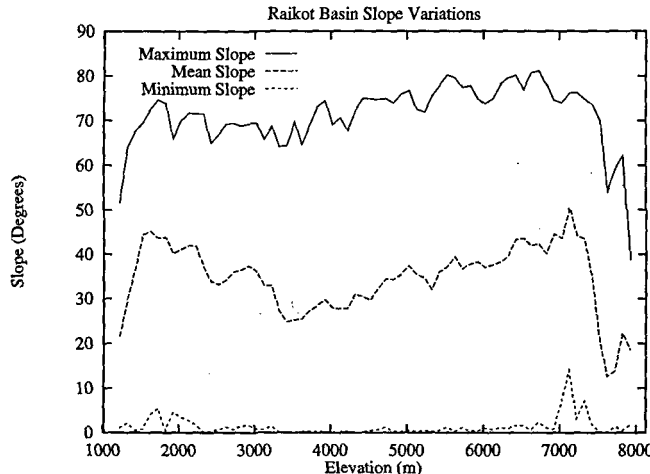


Figure 12 Slope-Altitude relationships for Raikot Basin. Slope statistics were calculated over an elevation range of 100 m. The relationship between slopes and altitude is not linear. Steep slopes can be found at all altitudes. Average slope angles decrease to a minimum at ≈ 3300 m due to the influence of glaciation. At higher elevations, the average slope angles increase due to a decrease in temperature (freeze-thaw action) and the dominance of mass movement.

Remote sensing of the surface and near surface has dramatically increased our capability to characterize and model sediment flux, assess geomorphological conditions, and assess the topographic evolution of this dynamic environment. In addition, remote sensing data and information are being used in quantitative modeling efforts to estimate denudation rates, test our model, and generate a model of topographic evolution.

Geomorphometric information generated from spatial analysis of the DEM has confirmed the removal of a significant amount of rock and sediment (Shroder *et al.*, 1998c). Results of hydrologic modeling indicate that mean fluvial denudation for several basins on the north side of Nanga Parbat is $\approx 7 \text{ mm yr}^{-1}$. These are the highest reported rates for the western Himalaya. Topographic analysis, coupled with temporal control from cosmogenic nuclide dating, has also verified rapid river incision that is partly responsible for steep slopes. Similarly, spatial analysis has been used to characterize the complexity of the topography. To date, we know that the topography has been significantly influenced by glaciation. Satellite image analysis, DEM analysis, and cosmogenic isotope exposure ages have enabled us to determine that the modern landscape is dominated by a glacial heritage from late Pleistocene and early Holocene. These results are quite significant as these time periods are associated with monsoon activity and indicate that glaciation was much more extensive in the past, playing a significant role in mass flux of sediment.

Remote sensing has played a significant role in assessing modern-day glaciers and estimating glacial denudation rates. Spatial analysis of multispectral satellite imagery can be used to assess the structural and sediment load characteristics on alpine glaciers in the Himalaya (Bishop *et al.*, 1998a). Similarly, the integration of data and information generated

from image analysis and field work enable accurate mapping, assessment of sediment load variability and transfer efficiency, and the estimation of glacial denudation rates (Bishop *et al.*, 1995; Bishop *et al.*, 1998b; Shroder *et al.*, 1998b). To date, results indicate that modern-day glacial denudation may be highly variable, although our results support work conducted by Gardner and Jones (1993). The integration of satellite imagery, digital elevation data, and field data is critical for estimating the magnitude of glacial denudation around the mountain.

Our working model has focused on the major surface processes responsible for rapid denudation (mass movement, fluvial, glacial). Remote sensing analyses, coupled with traditional analyses, have enabled us to rigorously test our working model and make refinements. For example, land cover and topographic features identifiable in satellite imagery and the DEM have led to the recognition of maximum ice conditions and the significance of catastrophic flooding. Similarly, we now recognize that denudation is highly variable in space and time and that differential denudation has produced the extreme relief at Nanga Parbat. Remote sensing and GIS analyses are playing a fundamental role in assessing the spatial variability of denudation resulting from a variety of processes.

Collectively, remote sensing and GIS technology have been and will continue to be fundamental in studying lithospheric processes. The integration of data has thus enabled a systematic approach to be used to study localized coupling between tectonic and surface processes at Nanga Parbat. We have discovered that intense local erosion has caused rapid exhumation of the massif, which in turn, has led to thermal weakening of the upper crust and consequent further concentration of strain (Zeitler, *et al.*, 1998). This new understanding, of what can be considered a kind of tectonic aneurysm, is a direct result of the integration of remote sensing, GIS, geophysics, and conventional field techniques. In future studies of this kind, it will become ever more important for geoscientists to integrate quantitative remote sensing and GIS into a standard analytical framework in order to solve complex problems.

Conclusions

The Nanga Parbat Project represents a multidisciplinary investigation of the relationships between tectonic and surface processes at the Nanga Parbat massif in northern Pakistan. Remote sensing and GIS technology play an important role in assessing subsurface and surface conditions as well as in the quantitative analysis and modeling of process rates. To date, remote sensing and GIS investigations have improved our current understanding of the topographic evolution of the massif. Remote sensing and GIS studies have been used to validate working models, and ongoing research will provide information that will further refine these models and provide new insights into the dynamic nature of mountain building. Unusual linkages between subsurface and surface processes have been discovered already in our analyses. Further work

of this kind here and in other areas is providing the scientific community with a new understanding of lithospheric processes in complex mountain environments.

Acknowledgments

This work was funded in part by the University Committee on Research at the University of Nebraska at Omaha, and the National Science Foundation (Grant No. EAR 9418839). We thank Martin Sharp and Peter Nienow for loan of the glacier surveying and radio-echo sounding equipment, and Andrew Elmore for his assistance in the field in 1996. We also thank Jeff Olsenholle for his contributions.

References

- Anderson, D.L. and A.M. Dziewonski, 1984. Seismic Tomography. *Scientific American*, October, 5464.
- Avouac, J.P. and E.B. Burov, 1996. Erosion as a Driving Mechanism of Intracontinental Mountain Growth, *Journal Geophysical Research*, 101: 17, 747-17,769.
- Bian, L., 1997. Multiscale Nature of Spatial Data in Scaling Up Environmental Models, in *Scale in Remote Sensing and GIS* Editors, D. A. Quattrochi and M. F. Goodchild, Lewis Publishers, New York, p. 13-26.
- Bishop, M.P., J.F. Shroder Jr., and J.L. Ward, 1995. SPOT Multispectral Analysis for Producing Supraglacial Debris-Load Estimates for Batura Glacier, Pakistan. *Geocarto International*, 10, 8190.
- Bishop, M.P., J.F. Shroder, Jr., B.L. Hickman, and L. Copland, 1998a, Scale Dependent Analysis of Satellite Imagery for Characterization of Glacier Surfaces in the Karakoram Himalaya, Special Volume on Remote Sensing in Geomorphology, Editors, S. Walsh and D. Butler, *Geomorphology*, 21, 217-232.
- Bishop, M.P., B.L. Hickman, and J.F. Shroder Jr., 1998b, in press. High Resolution Satellite Imagery and Neural Networks for Information Extraction in a Complex Mountain Environment, *Geocarto International*.
- Bogorodsky, V.V., C.R. Bentley, and P.E. Gudmandsen, 1985. *Radioglaciology*. Reidel, Dordrecht.
- Brozovik, N., D. Burbank, A.J. Meigs, 1997. Climatic Limits on Landscape Development in the Northwestern Himalaya, *Science*, 276, 571-574.
- Burbank, D., J. Leland, E. Fielding, R.S. Anderson, N. Brozovik, M. R. Reid, and C. Duncan, 1996. Bedrock Incision, Rock Uplift and Threshold Hillslopes in the Northwestern Himalayas, *Nature*, 379, 505-510.
- Butler, R.W.H. and D.J. Prior, 1988. Tectonic Controls on the Uplift of the Nanga Parbat Massif, Pakistan Himalayas, *Nature*, 333: 247-250.
- Cao, C. and N. Siu-Ngan Lam, 1997. Understanding the Scale and Resolution Effects in Remote Sensing and GIS, in *Scale in Remote Sensing and GIS* Editors, D. A. Quattrochi and M. F. Goodchild, Lewis Publishers, New York, 57-72.
- Chamberlain, C.P., P.K. Zeitler, D.E. Barnett, D. Winslow, S.R. Poulsen, T. Leahy, and J.E. Hammer, 1995. Active Hydrothermal Systems During Recent Uplift of Nanga Parbat, Pakistan Himalaya, *Journal of Geophysical Research*, 100, 439-453.

- Civco, D., 1989. Topographic Normalization of Landsat Thematic Mapper imagery, *Photogrammetric Engineering and Remote Sensing*, 55, 1303- 1309.
- Colby, J.D., 1991. Topographic Normalization in Rugged Terrain, *Photogrammetric Engineering and Remote Sensing*, 57, 531-537.
- Colby, J.D., and P.L. Keating, 1998, in press. Land Cover Classification Using Landsat TM Imagery in the Tropical Highlands: the Influence of Anisotropic Reflectance, *International Journal of Remote Sensing*.
- Corbel, J., 1959. Vitesse de l'Erosion. *Zeitschrift fur Geomorphologie* 1: 1-28.
- Coward, M.P., B.F. Windley, R.D. Broughton, I.W. Luff, M.G. Petterson, C.J. Pudsey, D.C. Rex, and M.A. Khan, 1986. Collision Tectonics in the Northwest Himalaya, in *Collision Tectonics*, Editors, Coward, M.P. and Ries, A.R., Geological Society London Special Publication 19: 203-219.
- DeFries, R. S., J. R. Townshend, and S. O. Los, 1997. Scaling Land Cover Heterogeneity for Global Atmosphere-Biosphere Models, in *Scale in Remote Sensing and GIS*, D. A. Quattrochi and M. F. Goodchild, Editors, Lewis Publishers, New York, 231-246.
- Dobrin, M.B., 1976. *Introduction to geophysical prospecting*. McGraw-Hill, 591-601.
- Ekstrand, S., 1996. Landsat TM-based Forest Damage Assessment: Correction for Topographic Effects, *Photogrammetric Engineering and Remote Sensing*, 62, 151 - 161.
- England, P. and P. Molnar, 1990. Surface Uplift, Uplift of Rocks, and Exhumation of Rocks, *Geology*, 18, 1173-1177.
- Estes, J.E. (editor), 1983, Manual of Remote Sensing: Second Edition, Vol. 2 (Falls Church, Virginia: The Sheridan Press).
- Evans, S., 1965. Dielectric Properties of Ice and Snow - a Review, *Journal of Glaciology*, 5, 773792.
- Finterswalder, R., 1937. Die Gletscher der Nanga Parbat, *Zeitschrift für Gletscherkunde und Eiszeiforschung und Geschichte des Klimas*, 25, 57-108
- Franklin, S.E., and B.A. Wilson, 1992. A Three-Stage Classifier for Remote Sensing of Mountain Environments, *Photogrammetric Engineering and Remote Sensing*, 58: 4, 449-454.
- Friedl, M. A., 1997. Examining the Effects of Sensor Resolution and Sub-Pixel Heterogeneity on Spectral Vegetation Indices: Implications for Biophysical Modeling, in *Scale in Remote Sensing and GIS*, Editors, D. A. Quattrochi and M. F. Goodchild, Lewis Publishers, New York, 113- 139.
- Gardner, J.S. and N.K. Jones, 1993. Sediment Transport and Yield at the Raikot Glacier, Nanga Parbat, Punjab Himalaya. in *Himalaya to the Sea*, Editor Shroder, J.F., Jr., Routledge, London. p. 184-197.
- Gong, P., 1996. Integrated Analysis of Spatial Data From Multiple Sources: Using Evidential Reasoning and Artificial Neural Network Techniques for Geological Mapping, *Photogrammetric Engineering and Remote Sensing*, 62: 5, 513-523.
- Hallet, B., L. Hunter, and J. Bogen, 1996. Rates of Erosion and Sediment Evacuation by Glaciers: a Review of Field Data and their Implications, *Global and Planetary Change*, 12: 213-235.
- Harbor, J. and J. Warburton, 1993. Relative Rates of Glacial and Nonglacial Erosion in Alpine Environments, *Arctic and Alpine Research*, 25: 1-7.
- Harrison, C.G., 1994. Rates of Continental Erosion and Mountain Building, *Geol. Rundsch.*, 83, 431-447.
- Hodgson, M.E., and B.M. Shelley, 1994. Removing the Topographic Effect in Remotely Sensed Imagery, *ERDAS Monitor*, 6, 4-6.
- Hoffman, P.F., and J.P. Grotzinger, 1993. Orographic Precipitation, Erosional Unloading, and Tectonic Style, *Geology*, 21, 195-198.
- Holben, B.N., and C.O. Justice, 1979. Evaluation and Modeling of the Topographic Effect on the Spectral Response from Nadir Pointing Sensors, *NASA Technical Memorandum* 80305, Greenbelt Maryland.
- Hugli, H., and W. Frei, 1983. Understanding Anisotropic Reflectance in Mountainous Terrain, *Photogrammetric Engineering and Remote Sensing*, 49, 671 -683.
- Justice, C.O., and B. Holben, 1979. Examination of Lambertian and Non-Lambertian Models for Simulating the Topographic Effect on Remotely Sensed Data, *NASA Technical Memorandum* 80557, Greenbelt, Maryland.
- Justice, C.O., S.W. Wharton, and B.N. Holben, 1980. Application of Digital Terrain Data to Quantify and Reduce the Topographic Effect on Landsat Data, *NASA technical Memorandum* 81988, Greenbelt, Maryland.
- Lawrence, R.D. and A.A.K. Ghauri, 1983. Evidence of Active Faulting in Chiulas District. *Geological Bulletin University of Peshawar, Pakistan*, 16: 185-186.
- Lawrence, R.D. and J.F. Shroder, Jr., 1984. Active Fault Northwest of Nanga Parbat. *First Pakistan Geological Congress Volume of Abstracts*, Lakore, Punjab University, 50-51.
- Madin, I., 1986. Structure and Neotectonics of the Northwestern Nanga Parbat - Haramosh Massif, *Unpublished M.S. thesis*, Oregon State University, Corvallis, Oregon.
- Masek, J.G., B.L. Isacks, T.L. Gubbels, and E.J. Fielding, 1994. Erosion and tectonics at the margins of continental plateaus, *Journal of Geophysical Research*, 99: 13,941-13,956.
- Meltzer, A., L. Seeber, J. Armbruster, and B. Beaudoin, 1998, in review. Seismicity and Fluid Flow at Active Metamorphic Massifs, Nanga Parbat, Pakistan Himalaya, *Science*.
- Meyer, P., K.I. Itten, T. Kellenberger, S. Sandmeier, and R. Sandmeier, 1993. Radiometric Corrections of Topographically Induced Effects on Landsat TM Data in an Alpine Environment, *Journal of Photogrammetry and Remote Sensing*, 48, 17-28.
- Minnaert, J.L., 1941. The Reciprocity Principle in Lunar Photometry, *The Astrophysics Journal*, 93, 403-410.
- Molnar, P. and P. England, 1990. Late Cenozoic Uplift of Mountain Ranges and Global Climate Change: Chicken or Egg? *Nature*, 346: 29-34.
- Montgomery, D.R., 1994. Valley Incision and the Uplift of Mountain Peaks, *Journal Geophysical Research*, 99: 13, 913-13,921.
- Narod, B.B. and G.K.C. Clarke, 1994. Miniature High-power Impulse Transmitter for Radio-echo Sounding, *Journal of Glaciology*, 40, 190- 194.
- Oswald, G.K.A., 1984. Ice-depth Radio Echo-sounding Techniques Employed on the Hispar and Ghulkin Glaciers, in *The International Karakoram Project*, Vol. 2, Editor Miller, K.J., Cambridge University Press, Cambridge, 86-99.
- Owen, L., 1988. Terraces, Uplift and Climate, Karakoram Mountains, Northern Pakistan, *Unpublished Ph.D. thesis*, University of Leicester, U.K.
- Park, S.K., and R.L. Mackie, 1998a, in press. Crustal Structure at

- Nanga Parbat, Northern Pakistan, from Magnetotelluric Soundings, *Geophysical Review Letters*.
- Park, S.K., and R.L. Mackie, 1998b, in review. Magnetotelluric Soundings at Nanga Parbat Lack Evidence for Crustal Fluids, *Science*.
- Paterson, W.S.B., 1994. *The Physics of Glaciers*, 3rd Edition, Edward Arnold Ltd.
- Pecknold, S., S. Lovejoy, D. Schertzer, and C. Hooge, 1997. Multifractals and Resolution Dependence of Remotely Sensed Data: GSI to GIS, in: *Scale in Remote Sensing and GIS* Editors D. A. Quattrochi and M. F. Goodchild, Lewis Publishers, New York, 361-394.
- Pillewizer, W., 1956. Der Rakhiot-Gletscher am Nanga Parbat im Jahre 1954, *Zeitschrift fur Gletscherkunde und Glazialgeologie*, 3, 181-194.
- Pinter, N. and M.T. Brandon, 1997. How Erosion Builds Mountains, *Scientific American*, April, 74-79.
- Quattrochi, D. A., N. Siu-Ngan Lam, H. Qiu, and W. Zhao, 1997. In: *Scale in Remote Sensing and GIS*, Editors, D. A. Quattrochi and M. F. Goodchild, Lewis Publishers, New York, 295-308.
- Raymo, R.E. and W.F. Ruddiman, 1992. Tectonic Forcing of Late Cenozoic Climate, *Nature*, 359: 117122.
- Sharma, P.V., 1986. *Geophysical methods in geology*, Elsevier, 322-329.
- Shroder, J.F., Jr., M.S. Khan, R.D. Lawrence, I. Madin, and S.M. Higgins, 1989. Quaternary Glacial Chronology and Neotectonics in the Himalaya of Northern Pakistan, in Tectonics and Geophysics of the Western Himalaya, *Geological Society of America Special Paper* 232, Editors, L.L. Malinconico, Jr. and R.J. Lillie, 275-293.
- Shroder, J.F., Jr., L. Owen, and E. Derbyshire, 1993. Quaternary Glaciation of the Karakoram and Nanga Parbat Himalaya, *Himalaya to the Sea*, Editor, Shroder, J.F., Jr., Routledge, London, 132158.
- Shroder, J.F., Jr. and M.P. Bishop, 1998a, in press. Mass Movement in the Himalaya: New Insights and Research Directions, *Geomorphology*.
- Shroder, J.F., Jr., M.P. Bishop, L. Copland, and V. Sloan, 1998b, in press. Debris-covered Glaciers and Rock Glaciers in the Nanga Parbat Himalaya, *Geografiska Annaler*.
- Shroder, J.F., Jr., M.P. Bishop, L. Copland, K.J. Cornwell, R.A. Marston, D. Norsby, W.M. Phillips, R. Scheppy, and V.F. Sloan, 1998c, in review. Differential Denudation Produces Extreme Relief, Nanga Parbat Himalaya, *Science*.
- Smith, J., T. Lin, and K. Ranson, 1980. The Lambertian assumption and Landsat data, *Photogrammetric Engineering and Remote Sensing*, 46, 1183- 1189.
- Teillet, P.M., B. Guindon, and D.G. Goodenough, 1982. On the Slope-aspect Correction of Multispectral Scanner Data, *Canadian Journal of Remote Sensing*, 8, 84-106.
- Treloar, P.J., D.C. Rex, P.G. Guise, M. P. Coward, M.P. Searle, B.F. Windley, M.G. Petterson, M.Q. Jan, and I.W. Luff, 1989. K-Ar and Ar-Ar Geochronology of the Himalayan Collision in NW Pakistan: Constraints on the Timing of Suturing, Deformation, Metamorphism and Uplift, *Tectonics*, 8: 881909.
- Zeitler, P.K., 1985. Cooling History of the Northwest Himalaya, *Tectonics*, 4: 127- 151.
- Zeitler, P.K. and C.P. Chamberlain, 1991. Petrogenetic and Tectonic Significance of Young Leucogranites from the Lorthwestern Himalaya, Pakistan, *Tectonics* 10: 729-741.
- Zeitler, P.K., C.P. Chamberlain, and H.A. Smith, 1993. Synchronous Anatexis, Metamorphism, and Rapid Denudation at Nanga Parbat (Pakistan Himalaya), *Geology* 21: 347-350.
- Zeitler, P.K., P.O. Koons, M.P. Bishop, C.P. Chamberlain, L. Copland, D. Craw, M.A. Edwards, P. Le Fort, S. Hamidullah, M. Qasim Jan, M. Asif Khan, M. Umar Khan, Khattak, W. Kidd, R.L. Mackie, A.S. Meltzer, S.K. Park, A. Pecher, W. Phillips, M. Poage, G. Sarker, D. Schneider, L. Seeber, J.F. Shroder, Jr., 1998, in review. Geodynamics of the Nanga Parbat Massif, Pakistan: The Geomorphology of Metamorphism, *Science*.

U.SVMexico border: Salton sea and Imperial valley, California and Mexicali



Space Shuttle Discovery February, 1994.

(NASA Photo STS60-101-038. Courtesy of Dr. Kamlesh Lulla, Earth Science Branch, NASA/
Johnson Space Center, Houston, Texas 77058, U.S.A.)